# A variational assimilation ensemble and the spatial filtering of its error covariances: increase of sample size by local spatial averaging

**Loïk Berre[*], Olivier Pannekoucke[*], Gérald Desroziers[*], Simona Ecaterina Ştefănescu[+], Bernard Chapnik[*] and Laure Raynaud[*]**

[*] *Météo-France, CNRM/GAME-GMAP, Toulouse, France*
[+] *National Meteorological Administration, LMN, Bucharest, Romania*

Abstract:

An ensemble of perturbed assimilations is a powerful technique to simulate the space and time dynamics of errors in an operational assimilation system. Using an ensemble of variational assimilations is relatively straightforward, as its basic elements can be directly derived from the operational variational scheme. Moreover, with respect to the analysis update of the perturbations, the potential benefit is both to adequately simulate the effect of the operational variational gain matrix, and to take advantage of its realism (e.g. non linear mass/wind balances), of its appropriate filtering, and of its full rank.

This includes available spectral and wavelet covariance tools also, which are believed to ease both an optimal estimation of filtered (possibly hybrid) ensemble covariances, and their use in the construction of the analysis members (including a careful filtering of sampling noise). It is also noticed that with e.g. an ensemble of 3D-Fgat, the analysis part of the assimilation ensemble cost is relatively small, compared to the forecast part.

In order to reduce the amplitude of sampling noise, local spatial averaging can be applied, as it allows the ensemble size to be multiplied by a 2D spatial sample size. A methodology, based on the comparison of statistics of two independent ensembles which have the same size, is also presented to estimate signal and sampling noise statistics. It is shown that the spatial structure of sampling noise is relatively small scale. This justifies the application of spatial filtering.

Following the usual linear estimation theory, it is shown that signal-to-noise ratios can be used also as objective and optimal filtering coefficients. The results indicate that a small ensemble (with typically 3 to 10 members) can provide relevant and robust information about flow-dependent error standard deviations, with e.g. larger values near troughs than near ridges. Comparison with innovation-based estimates and impact experiments tend to support these results. The (expected and effective) localized and positive nature of the flow-dependent modifications and impacts is also shown.

The use of wavelets for correlation modelling can also be seen as a spatial filtering tool applied to raw ensemble correlations, in order to improve their accuracy. These attractive filtering properties are illustrated too.

# 1 The variational assimilation ensemble at Météo-France

## 1.1 Simulating the error evolution of a reference assimilation cycle

Using an ensemble of perturbed assimilations is now relatively usual, in order to estimate e.g. climatological error covariances, which can be specified in variational assimilation schemes for instance (e.g. Houtekamer et al 1996, Fisher 2003, Buehner 2005, Berre et al 2006). These climatological estimates may include not only globally averaged covariances, but also local standard deviations, whose impact has been shown to be positive in Belo Pereira and Berre (2006).

The idea is to simulate the error evolution of the reference assimilation system (e.g. the operational 4D-Var assimilation cycle), by (explicitly or implicitly) perturbing observations and the background, in order to estimate the corresponding error covariances. Compared e.g. to the NMC method (Parrish and Derber 1992, Rabier et al 1998), one of the strengths of this approach is the ability to simulate the analysis effect in the error evolution (Berre et al 2006), and in particular the data density and the effect of the (sub-optimal) gain matrix of the reference system.

This can be illustrated by noting that the same basic equation and sub-optimal gain matrix $\mathbf{K}$ are involved in the equations for the analyzed state $\mathbf{x_a}$, for the exact state $\mathbf{x}_\star$, and for the analysis error $\mathbf{e_a} = \mathbf{x_a} - \mathbf{x}_\star$:

$$\mathbf{x_a} = (\mathbf{I} - \mathbf{KH})\mathbf{x_b} + \mathbf{Ky}$$

$$\mathbf{x}_\star = (\mathbf{I} - \mathbf{KH})\mathbf{x}_\star + \mathbf{Ky}_\star$$

$$\mathbf{e_a} = (\mathbf{I} - \mathbf{KH})\mathbf{e_b} + \mathbf{Ke_o}$$

where $\mathbf{y}_\star = \mathbf{Hx}_\star$, and where the third equation is simply deduced from the difference between the first two equations. This analysis error equation indicates that, when simulating the error evolution of the reference system, one should use the reference (sub-optimal) gain matrix $\mathbf{K}$ to transform observation and background perturbations into analysis perturbations. This is exactly what the ensemble of assimilations allows to be done, by implicitly handling differences $\varepsilon_\mathbf{a}$ between analyses which use this reference gain matrix $\mathbf{K}$:

$$\varepsilon_\mathbf{a} = (\mathbf{I} - \mathbf{KH})\varepsilon_\mathbf{b} + \mathbf{K}\varepsilon_\mathbf{o}$$

Moreover, it remains possible to incorporate e.g. flow-dependent ensemble information in this reference $\mathbf{K}$ matrix, for both deterministic and perturbed assimilations (see section 1.3 also). Thus, in the remainder of this paper, it will be suggested that, with respect to the construction of the analysis members, combining an ensemble of variational assimilations and spatial filtering tools may be an efficient approach, in order both to adequately simulate the analysis error step and to optimally filter sampling noise.

## 1.2 Design of the variational ensemble

Following the aforementioned studies on climatological covariance estimates, a real time variational assimilation ensemble is under development at Météo-France, in order to estimate flow-dependent covariances (as a next logical step). One of the main issues is naturally to decide about strategies with respect to the ensemble size and cost. The design of the ensemble has thus been guided by the following elements.

Firstly, it has been noticed that a small number of members (e.g. 3 to 10) already provides a lot of robust and interesting information. This will be shown e.g. in section 3, and it has been illustrated by Kucukkaraca and Fisher (2006) also.

Moreover, this robustness may be further enhanced by using spatial ergodic properties, in a similar way as in the domain of turbulence (with temporal ergodic properties, see e.g. Monin and Yaglom 1971). The idea is to increase the sample size, by calculating a local spatial average.

Another natural idea is that the full (reference) assimilation system may be approximated for the purpose of the error simulation. This is often achieved by lowering the model resolution, but one may also consider to approximate the assimilation scheme (e.g. by approximating 4D-Var with 3D-Fgat).

Based on these ideas, six global assimilation members are running in nearly real time at Météo-France. They are based on the Arpège model (Courtier and Geleyn 1988), with truncation T359, a stretching factor equal to $c = 1$ (uniform resolution), 46 vertical levels and 3D-Fgat.

Diagnostic studies have indicated that e.g. standard deviation maps were relatively similar between the 3D-Fgat and 4D-Var ensembles, as in particular they reflect the weather situation (e.g. positions of troughs and ridges) and data density effects (plus effects of common parts of the variational gain matrix).

With such a configuration, the cost of the assimilation ensemble is similar to the cost of the operational 4D-Var cycle at Météo-France (with T359 c2.4 L46 for high resolution trajectories). This rather small cost of the assimilation ensemble reflects also the fact that in the 3D-Fgat ensemble, the analysis cost is relatively small, compared to the forecast cost. In other words, running an assimilation ensemble is not much more costly than simply running a forecast ensemble.

Moreover, 3D-Fgat is easy to build from the operational 4D-Var configuration, as the basic elements of 3D-Fgat can be directly derived from 4D-Var. In addition, this configuration will make it easy in the future to consider possible intermediate configurations between 3D-Fgat and the full operational 4D-Var (e.g. an ensemble of 4D-Var with a reduced number of minimizations).

It may be also mentioned that this global assimilation ensemble has provided lateral boundary conditions, during two experimental periods of two weeks, to a regional ensemble with the Aladin limited area model (at 10 km resolution). This Aladin ensemble has provided initial and lateral boundary conditions to a high resolution ensemble with the Arome model at 2.5 km resolution. The results (Desroziers et al 2007) indicate the ability of these ensembles to reflect expected seasonal contrasts in the covariances.

### 1.3 Comparison with an ETKF-Var hybrid scheme

It may be of interest to compare such a variational assimilation ensemble with a hybrid ETKF-Var scheme, with respect to the gain matrix to be used for the analysis update of the perturbations. In such a hybrid ETKF-Var scheme, the ETKF (Bishop et al 2001) is used to determine how background perturbations are to be updated into analysis perturbations. The corresponding **B** matrix is in fact solely derived from the available ensemble of backgrounds, without any representation of the effect of the actual gain matrix used in the reference 4D-Var run (except for observation operators, which can be taken from 4D-Var).

In contrast, in a variational assimilation ensemble, the gain matrix for the analysis perturbation update adequately represents the actual operators used in the **B** matrix of 4D-Var (e.g. non linear balances, standard deviations and correlations, either climatological, or flow-dependent, or hybrid). In fact, the 3D-Fgat variational gain matrix can still incorporate flow-dependent ensemble information, either in the form of extra control variables (Lorenc 2003, Buehner 2005), or in the standard deviations and correlations (with possibly optimized spatial filtering, as will be shown later on). The potential benefit of the variational assimilation ensemble corresponds thus also to the realism of e.g. non-linear mass/wind balances (Fisher 2003), to the full rank of the

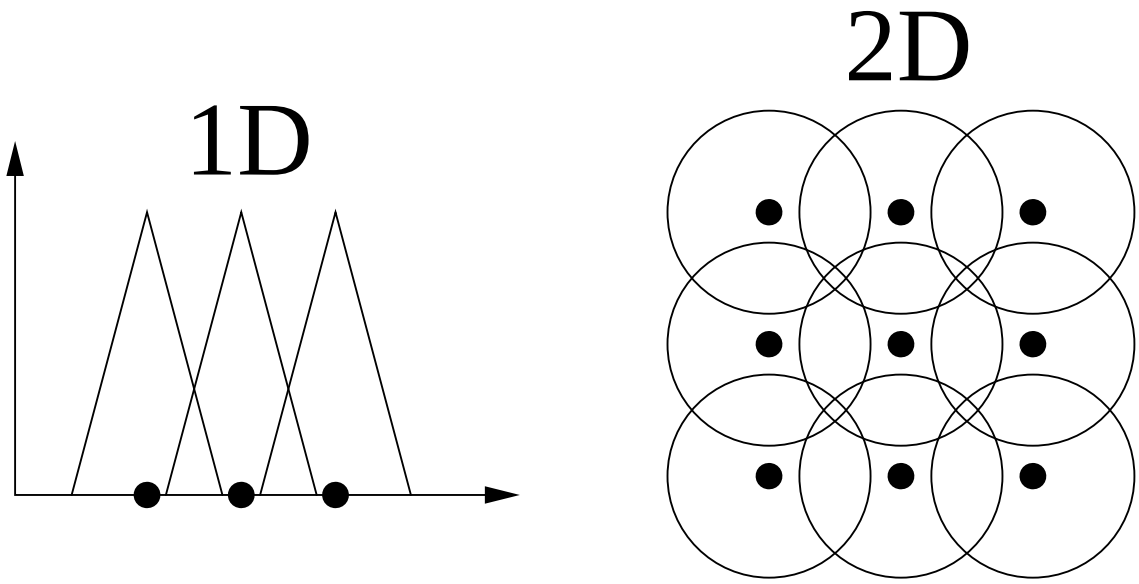


*Figure 1: Visualization of the number $N_g$ of nearest gridpoints in simple 1D ($N_g = 3$) and 2D ($N_g = 9$) cases. In 1D, the curves correspond to (simplified) correlation functions. In 2D, the isolines correspond to the distance at which the background error correlation is close to zero.*

covariances, and to their optimization facilities.

A common feature is that in both cases, the cost of the assimilation ensemble is more or less dominated by the cost of the forecast (while the analysis part is relatively costless). As mentioned previously, the variational framework offers the possibility also to consider intermediate configurations between 3D-Fgat and 4D-Var in the assimilation ensemble.

## 2 The concept of local spatial averaging

### 2.1 Increase of sample size

Said shortly, the basic idea is to MULTIPLY(!) the ensemble size $N_e$ by a number $N_g$ of gridpoint samples, to define a total sample size $N_t = N_e \times N_g$ (over which covariances are calculated).

The simplest case of a local gridpoint average is illustrated in Figure 1 for the 1D and 2D cases, by considering an average over the nearest gridpoints. In the 1D case, $N_g = 3$, while in the 2D case, $N_g = 9$. This means for instance that if $N_e = 6$, then the 2D total sample size will be equal to $N_t = 9 \times 6 = 54$. This corresponds to an increase by almost one order of magnitude.

Depending on the parameter and configuration, it may be also considered to calculate a spatial average over a larger number of gridpoints. Thanks to the 2D geometry on one hand, and because the increase is obtained through a multiplication of $N_e$ by $N_g$ (instead of a simple addition for instance), the increase of sample size can be quite large.

Another attractive feature is that this kind of spatial averaging can be performed efficiently in spectral space, through a costless multiplication by a low-pass filter. This corresponds to the classical equivalence between a multiplication in spectral space and a convolution in gridpoint space (see e.g. Courtier et al 1998, in a different but related context over the sphere).

## 2.2 Conditions at play

An ideal case for the relevance and efficiency of this local averaging arises from two basic conditions. A first condition is that the statistic of interest (e.g. either the standard deviation, or the correlation, or both) should be nearly homogeneous locally, or at least (more or less) slowly varying. This will ensure that the local spatial average remains representative of the gridpoint statistic of interest.

A second condition is that the background error correlation length-scales are relatively short. This will ensure that the neighbouring gridpoint error realizations are nearly independent, so that there is an effective increase of the number of independent samples (when locally averaging).

If one considers e.g. the estimation of local standard deviations, a synthesis of these two conditions may be expressed as follows. The spatial average is particularly efficient when the typical scales (of geographical variations) of the standard deviation field are larger than the background error correlation length-scales.

Another way to justify spatial filtering is to notice that, experimentally, the sampling noise tends to be relatively small scale, compared to the signal of interest. This is shown e.g. in Figure 6 of Fisher and Courtier (1995) in a simple 1D academic context. This small scale structure of sampling noise will be diagnosed and illustrated here in a real NWP context.

It may be also anticipated that the second condition amounts to considering that the sampling noise correlation length-scale is relatively small. This corresponds to the idea that the sampling noise values (on e.g. the ensemble gridpoint standard deviations) for two neighbouring gridpoints will tend to be uncorrelated, if the associated background error realizations are also uncorrelated (when considering sampling noise as a random process, essentially driven by the random values of the background perturbations).

This can be seen as a connection with the design of an objective and optimal filter, which will be evoked later on: an ideal condition is when the scales (of geographical variations) of the standard deviation field are larger than the typical scales of sampling noise. As will be illustrated below, experimental results suggest that these conditions are nearly met in practice.

## 2.3 Illustration in a simulated framework

One way to illustrate and understand the properties of sampling noise and of local spatial averaging is to consider a simulated framework, in which a true state can be defined, handled and compared to.

This has been achieved by considering the randomization (Fisher and Courtier 1995, Andersson and Fisher 1998) of the operational version of the Arpège background error covariance matrix. This operational version includes background error standard deviations for vorticity, which vary geographically (according to a climatological average from an ensemble of assimilations (Belo Pereira and Berre 2006)).

These geographical variations are illustrated near the surface in the top left panel of Figure 2. As expected, the error standard deviations are larger over oceanic storm track areas (in the Northern Atlantic, in the Northern Pacific, and in the Southern Hemisphere), and they are smaller over data dense areas such as Northern America and Europe.

The right panels correspond to raw results of the randomization, calculated respectively from 6 and 220 random realizations. One first striking feature is that even with a small 6 member ensemble, it is possible to recognize the main large scale relevant features. On the other hand, for both 6- and 220-member ensembles, residual errors are also noticeable, and the second striking feature is that these (sampling) errors tend to be relatively

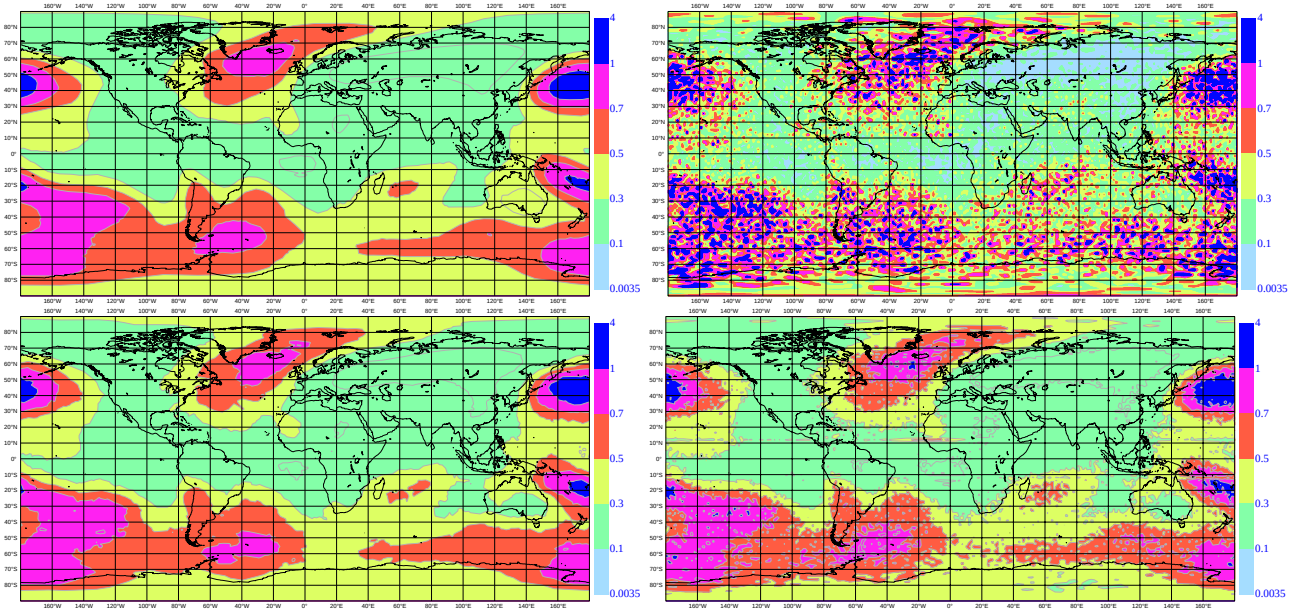

*Figure 2: Reference map of background error standard deviations (top left panel) and its randomized estimates: raw estimate with 6 members (top right panel), filtered estimate with 6 members (bottom left panel), and raw estimate with 220 members (bottom right panel). Unit:* $10^{-5}s^{-1}$.

small scale (with a larger amplitude when the ensemble is smaller, as expected). In other words, these two features illustrate the fact that the sampling noise is relatively small scale, compared to the signal of interest.

The bottom left panel corresponds to a spatially filtered version of the 6-member standard deviation map (which has been optimized "manually" in this case). As expected, the filtering removes small scale noise, while it preserves the large scale signal of interest. It may be also noticed that this filtered 6-member estimate tends to be even more accurate than the raw 220-member estimate. This increased accuracy reflects the fact that the total sample size $N_t$ of the filtered 6-member estimate is larger than the ensemble size of the raw 220-member estimate.

These results illustrate the potential efficiency of the local spatial averaging. On the other hand, one may wonder if it is possible to objectively diagnose and optimally filter out the amount of sampling noise in the context of a real ensemble of assimilations. This is the object of the next section.

# 3 Spatial filtering of local standard deviations

## 3.1 Illustration of signal and noise in a real ensemble of assimilations

A specific methodology has been applied, in order to diagnose the respective amounts of signal and of sampling noise, in a real ensemble of assimilations. The main idea is to compare statistics of two independent ensembles of assimilations which have the same size. Typically, from a first qualitative point of view, their common features can be seen as corresponding to the signal, while their differences correspond to effects of sampling noise.

The results for standard deviation maps are illustrated in Figure 3, for the case of two independent 3-member ensembles. It is striking that similar large scale structures are visible in the two maps, despite the small ensemble size. For instance, small values are visible in the North Atlantic ridge, while values larger by a factor of 2 or 3 can be seen in the neighbouring trough.

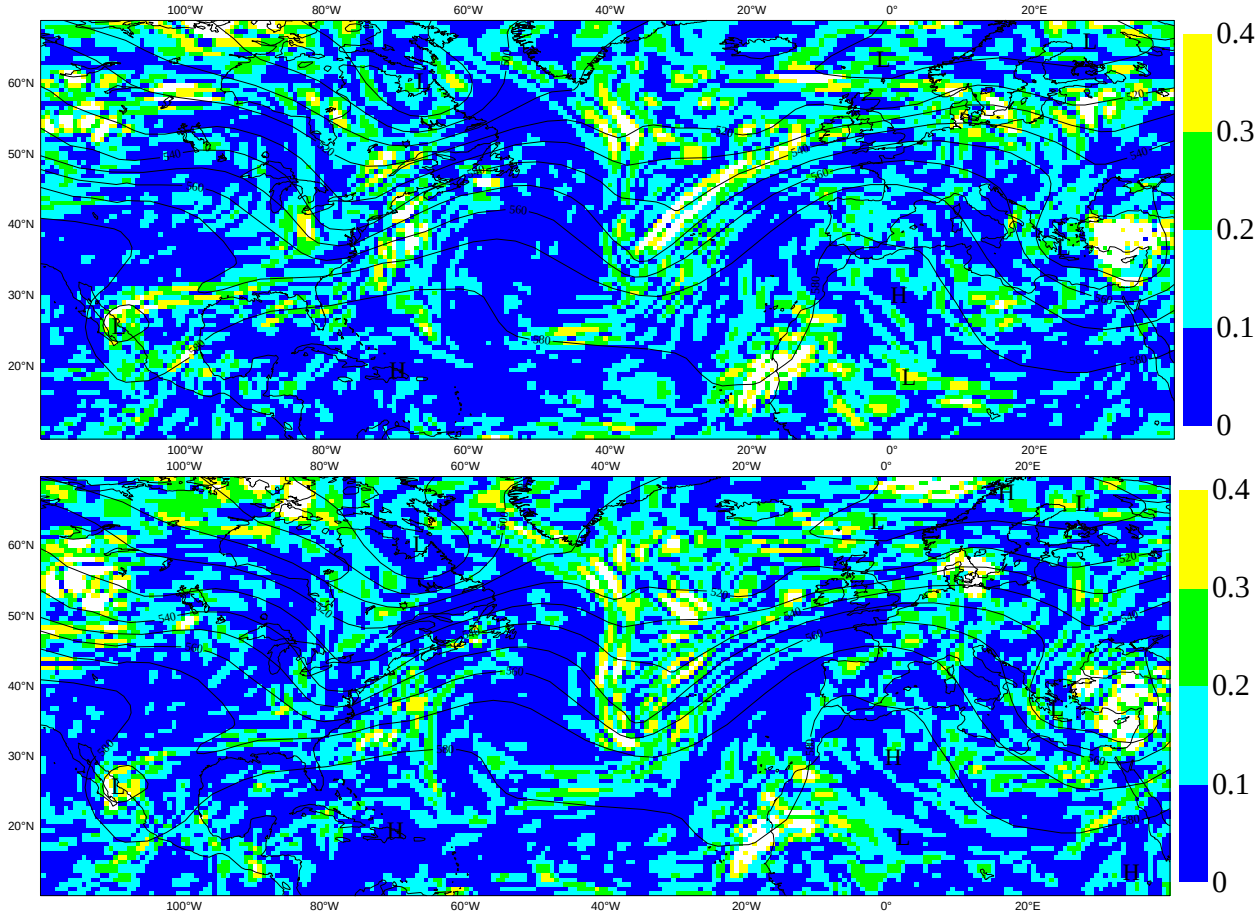


*Figure 3: Respective maps of raw standard deviations of vorticity near 500 hPa, derived from two independent three-member ensembles, valid for 11 February 2002 at 12 UTC. Unit:* $10^{-4}s^{-1}$.

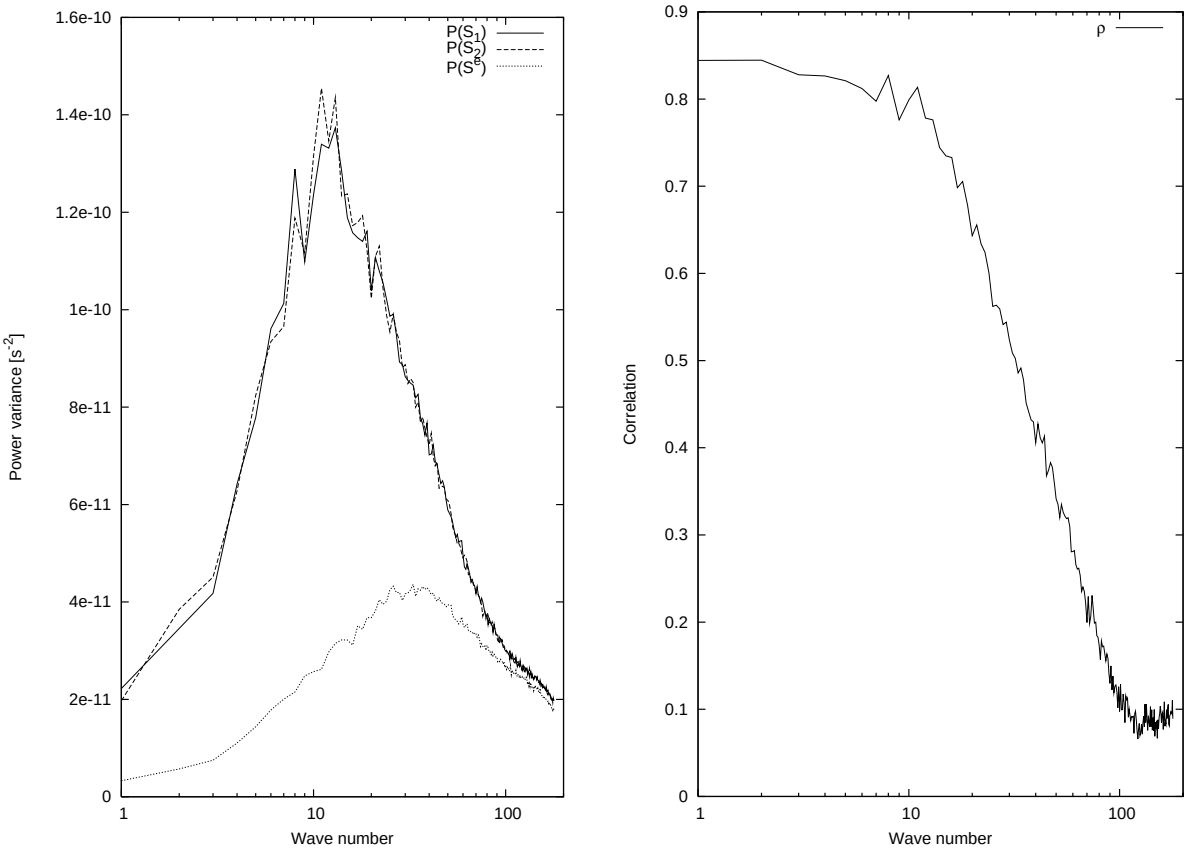


*Figure 4: Left panel: power spectra of daily variations of the raw standard deviation field of the first ensemble, namely* $\mathbf{P}(\mathbf{S}_1)$ *(full line), of the second ensemble, namely* $\mathbf{P}(\mathbf{S}_2)$ *(dashed line), and of sampling noise* $\mathbf{P}(\mathbf{S}^e)$ *(dotted line). The difference between the first two curves and* $\mathbf{P}(\mathbf{S}^e)$ *corresponds to the signal power* $\mathbf{P}(\mathbf{S}_\star)$*. Right panel: correlation* $\boldsymbol{\rho}$ *between the two ensemble-estimated maps of standard deviation, as a function of total wave number n.*

Conversely, one can also identify small scale details which do not coincide between the two maps. This suggests that the sampling noise is relatively small scale, compared to the signal of interest.

### 3.2 Formalism and diagnosis of signal and noise

To confirm this, one can try to estimate the amplitude (i.e. variance) of signal and noise, e.g. over a given time period (a 49-day period here, although a single day period could be enough as well). Formally, the standard deviation field $\mathbf{S}_i$ of the $i$th ensemble ($i$ =1 or 2) can be decomposed as:

$$\mathbf{S}_i = \mathbf{S}_\star + \mathbf{S}_i^e,$$

where $\mathbf{S}_i^e$ is the sampling error, and $\mathbf{S}_\star$ is the noise-free signal. Under the assumption that the sampling noise is a random process (arising from the randomness of observation perturbation values basically), it is uncorrelated with the signal. The variance of $\mathbf{S}_i$ may thus be decomposed as follows:

$$\mathbf{V}(\mathbf{S}_i) = \mathbf{V}(\mathbf{S}_\star) + \mathbf{V}(\mathbf{S}^e) \tag{1}$$

after noticing that $\mathbf{V}(\mathbf{S}_1^e) = \mathbf{V}(\mathbf{S}_2^e)$ (as the two independent ensembles have the same size), which may thus be noted $\mathbf{V}(\mathbf{S}^e)$. This noise variance may be estimated by expanding the difference between the ensemble estimates:

$$\mathbf{S}_1 - \mathbf{S}_2 = (\mathbf{S}_\star + \mathbf{S}_1^e) - (\mathbf{S}_\star + \mathbf{S}_2^e) = \mathbf{S}_1^e - \mathbf{S}_2^e,$$

and thus, under the assumption that the two noises $\mathbf{S}_1^e$ and $\mathbf{S}_2^e$ are two random uncorrelated processes: $\mathbf{V}(\mathbf{S}_1 - \mathbf{S}_2) = \mathbf{V}(\mathbf{S}_1^e) + \mathbf{V}(\mathbf{S}_2^e) - 2\ \mathbf{cov}(\mathbf{S}_1^e, \mathbf{S}_2^e) = 2\ \mathbf{V}(\mathbf{S}^e)$. This means that the noise variance can be estimated as half the variance of $\mathbf{S}_1 - \mathbf{S}_2$:

$$\mathbf{V}(\mathbf{S}^e) = \frac{1}{2}\mathbf{V}(\mathbf{S}_1 - \mathbf{S}_2)$$

While the above formalism is general, it is convenient to consider it in terms of spectral coefficients of the standard deviation maps, in order to diagnose the scale dependence of the signal and noise contributions. The individual modal variances $V(S_i(n,m))$ can be cumulated as a function of total wave number $n$, to provide the power spectrum $\mathbf{P}(\mathbf{S}_i)$: $P(S_i)[n] = \sum_{m=-n}^{+n} V(S_i(n,m)) = (2n+1)V(S_i)[n]$ (where $V(S_i)[n]$ is the average modal variance).

This power spectrum describes the total contribution of each wave number $n$ to the time variations of the estimated standard deviation field. The left panel of Figure 3 shows the power spectra associated to the two ensembles, $\mathbf{P}(\mathbf{S}_1)$ and $\mathbf{P}(\mathbf{S}_2)$. These two spectra are nearly identical, in accordance with equation (1).

The corresponding power spectrum of sampling noise $\mathbf{P}(\mathbf{S}^e)$ is also shown in this panel (dotted curve). Note also that, according to equation (1), the difference between the first two curves and the third one ($\mathbf{P}(\mathbf{S}^e)$) corresponds to the power of signal $\mathbf{P}(\mathbf{S}_\star)$. It appears that the amount of noise is relatively small in the large scales (where the largest time variations of the standard deviation fields occur), and that it is relatively large in the small scales.

Another way to visualize this scale dependence is to calculate the correlation between the two standard deviation maps, which is a simple function of the noise-to-signal ratio:

$$\rho = \frac{\mathbf{cov}(\mathbf{S}_1, \mathbf{S}_2)}{\sqrt{\mathbf{P}(\mathbf{S}_1)\mathbf{P}(\mathbf{S}_2)}} = \frac{\mathbf{P}(\mathbf{S}_\star)}{\mathbf{P}(\mathbf{S}_\star) + \mathbf{P}(\mathbf{S}^e)} = \frac{\mathbf{1}}{\mathbf{1} + \frac{\mathbf{P}(\mathbf{S}^e)}{\mathbf{P}(\mathbf{S}_\star)}}. \tag{2}$$

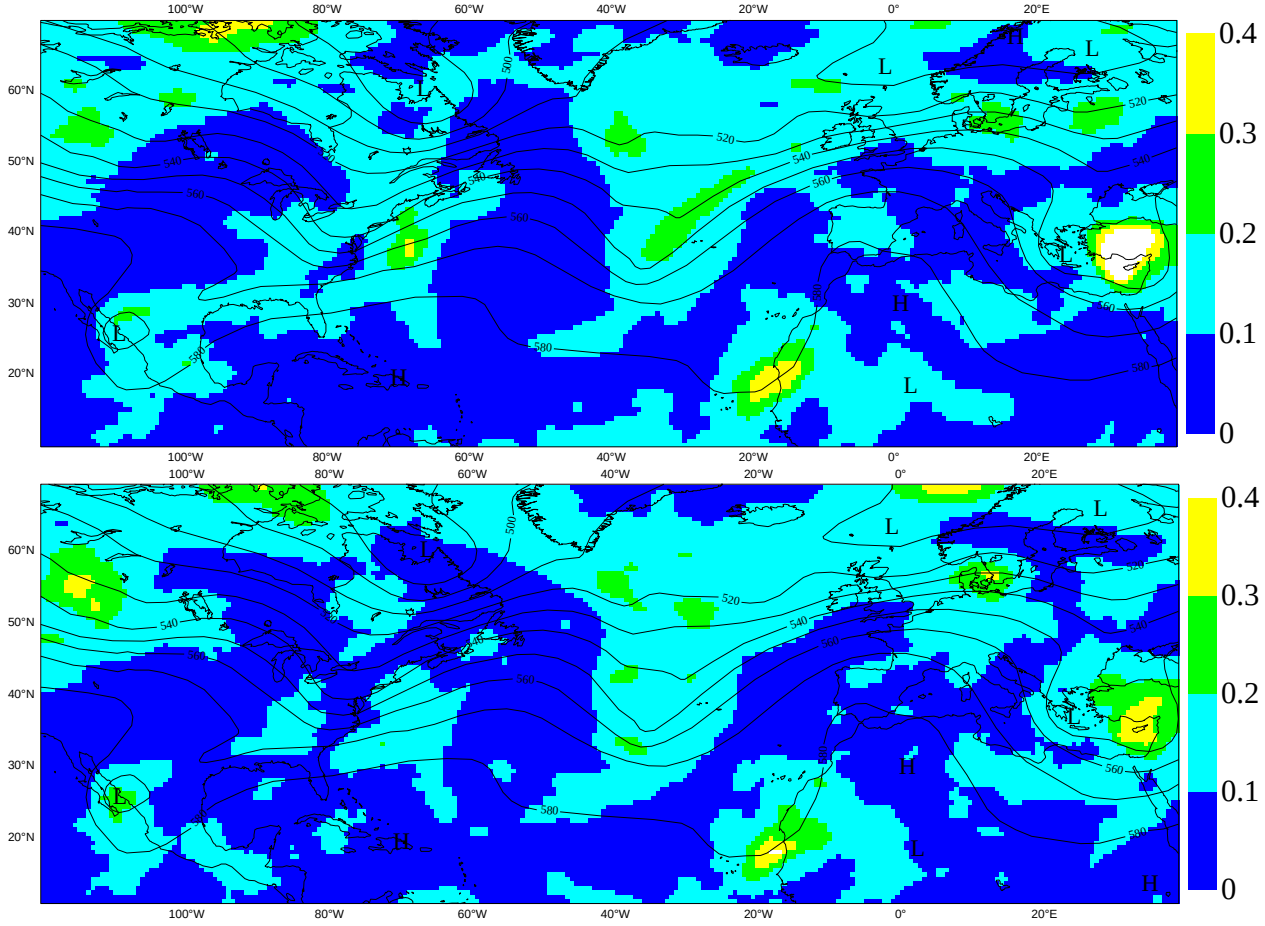


*Figure 5: Same as figure 3, after applying the objective and optimal filter. Unit:* $10^{-4}s^{-1}$.

The scale dependence of this correlation is shown in the right panel of Figure 4. It is larger than 80% in the large scales, and then it decreases progressively towards small values in the small scales.

These results in Figure 4 are consistent with expectations evoked in the previous section about Figure 3. This is also coherent with studies at ECMWF (Lars Isaksen, personal communication and this volume), showing that a 10-member standard deviation map estimate is similar to a 50-member estimate, except for some small scale sampling noise that could be filtered. All this supports the idea to apply a spatial filter, in order to extract the relevant large scale signal and to remove the small scale sampling noise.

### 3.3 Design and application of an objective and optimal filter

In order to design an objective and optimal filter, a simple idea is to apply the usual linear estimation theory (which is e.g. at the basis of most data assimilation techniques). A given ensemble estimate $\mathbf{S}_1$ can be seen as a predictor of the signal $\mathbf{S}_\star$, and formally, the best linear estimate of $\mathbf{S}_\star$ is provided by a simple regression equation (with the signal as the predictand):

$$\mathbf{S}_\star \sim \frac{\mathbf{cov}(\mathbf{S}_\star, \mathbf{S}_1)}{\mathbf{V}(\mathbf{S}_1)} \mathbf{S}_1.$$

and then it can be shown easily that the regression coefficent is simply equal to the correlation $\rho$ between the two ensemble estimates $\mathbf{S}_1$ and $\mathbf{S}_2$:

$$\frac{\mathbf{cov}(\mathbf{S}_\star, \mathbf{S}_1)}{\mathbf{V}(\mathbf{S}_1)} = \frac{\mathbf{V}(\mathbf{S}_\star)}{\mathbf{V}(\mathbf{S}_\star) + \mathbf{V}(\mathbf{S}^e)} = \frac{\mathbf{1}}{\mathbf{1} + \frac{\mathbf{V}(\mathbf{S}^e)}{\mathbf{V}(\mathbf{S}_\star)}} = \boldsymbol{\rho}$$

according to equation (2). This means that the correlation $\boldsymbol{\rho}$ is not only a useful diagnostic function of the signal-to-noise ratio. It can be also used as an objective and optimal filter of the raw ensemble standard deviation fields.

The results of this optimal filtering are illustrated in Figure 5, which can be compared to Figure 3. As expected, large scale coherent structures are extracted, while small scale noisy details tend to be removed.

It may be also mentioned that the amplitude of the regression residual error can be estimated, according to: $\mathbf{V}(\boldsymbol{\rho}\mathbf{S}_1 - \mathbf{S}_\star) = \boldsymbol{\rho}\ \mathbf{V}(\mathbf{S}^e)$. This equation and the corresponding results (not shown) indicate that the error reduction (achieved by the regression) is particularly large in the medium and small scales (in accordance with the shape of $\boldsymbol{\rho}$).

### 3.4 Comparison with innovation-based diagnostics

One way to validate ensemble standard deviation estimates is to compare them with independent estimates, derived from innovation data. In particular, it has been shown by Desroziers et al (2005) that the covariance between the analysis increment $\mathbf{dx}$ (in observation space) and the innovation $\delta\mathbf{y}$ is an estimate of the background error covariance (in observation space):

$$\mathbf{cov}(\mathbf{H}\ \mathbf{dx}, \delta\mathbf{y}) \sim \mathbf{HBH^T}.$$

An example of such a comparison is shown in Figure 6, for a specific date. Note that a simple spatial average has been applied to both ensemble and innovation-based estimates, with a 500 km averaging radius around each observation location. Moreover, as the ensemble standard deviations tend to be larger by a factor 1.4 (on the average) than the innovation-based estimates, the ensemble estimates have been divided by this factor, in order to focus on the comparison of geographical variations.

It is striking that similar spatial structures are visible in the two estimates, with e.g. large values in the Western Pacific, and smaller values in the Southern Atlantic. This relative coherence between these two independent estimates looks rather encouraging. This kind of comparison is believed to be essential in order to validate the ensemble estimates, and/or in order to improve their realism. In particular, as suggested by Daley (1992), such comparisons could provide objective information about model error covariances for instance.

### 3.5 Expected impacts and effective results

The current operational version of the Arpège 4D-Var experiments uses climatological ensemble standard deviations (as described in Belo Pereira and Berre 2006). In order to anticipate expected impacts of flow-dependent ensemble standard deviations (”of the day”), it is useful to compare examples of the corresponding maps (Figure 7).

It can be noticed firstly that there are similar large scale contrasts in the two maps, with e.g. larger values over the oceanic storm track areas, and smaller values e.g. in the tropics and over the data dense USA. It appears in fact that the strongest modifications of standard deviations are relatively localized spatially. They correspond to increases in local areas such as the Western part of the Northern Pacific, near the Southern coast of Australia, and Western Europe (which coincides with an intense storm over Northern France).

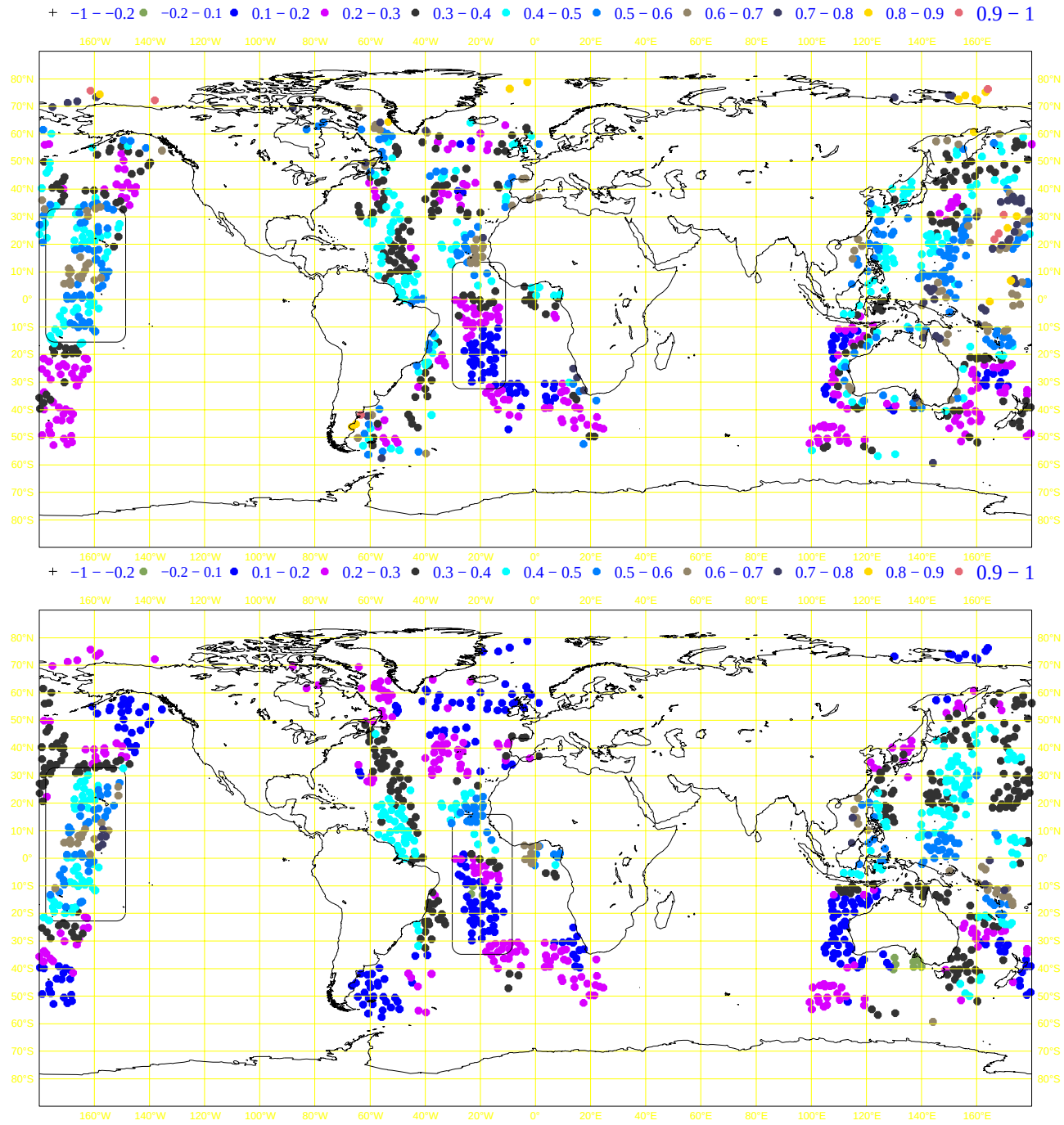


*Figure 6: Filtered background error standard deviations for channel HIRS 7, at available observation locations, for one specific date (28/08/2006 at 00h). Top panel: from a six member assimilation ensemble. Bottom panel: from the method based on covariances of residuals. Unit: K.*

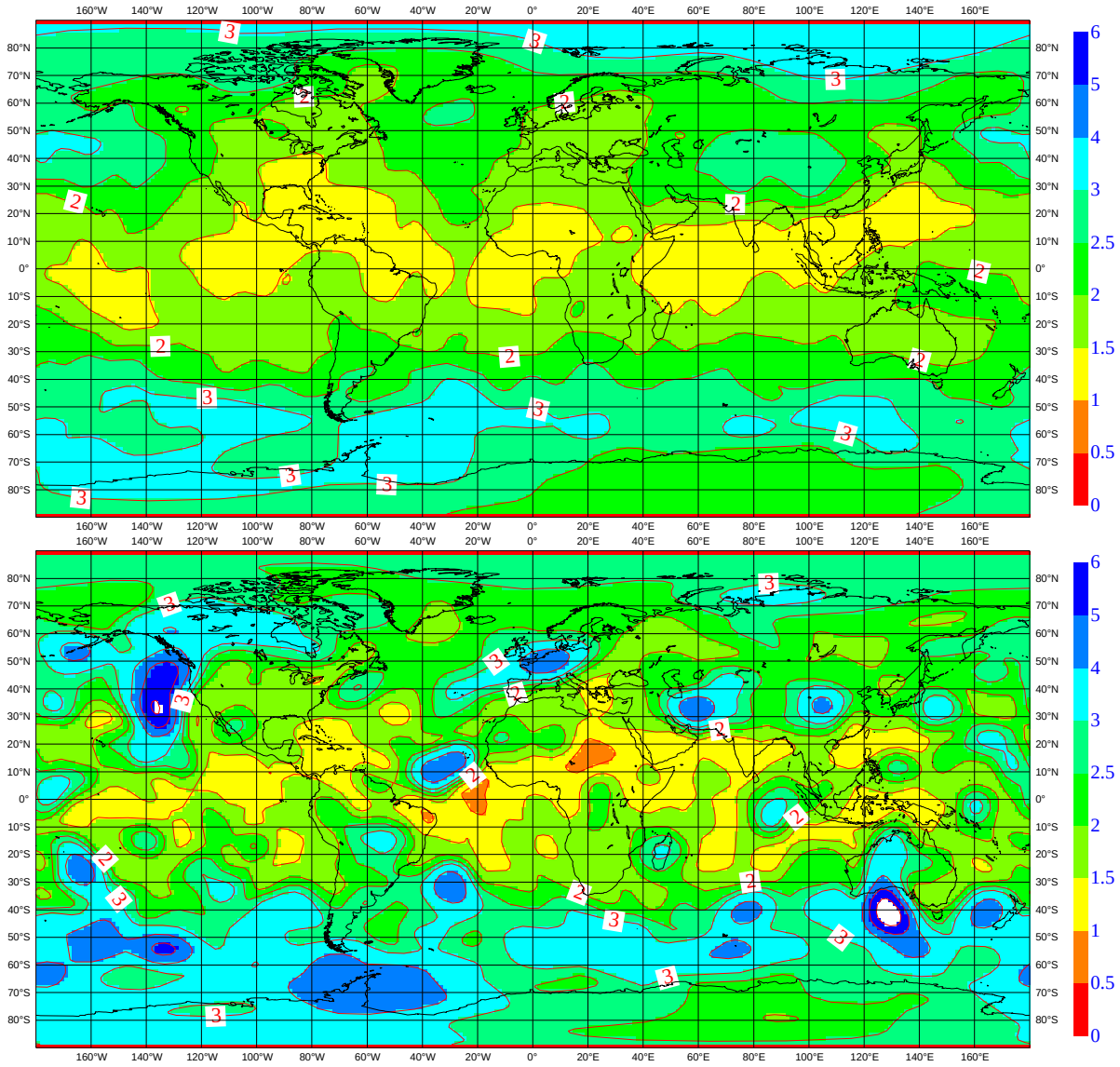


*Figure 7: Maps of standard deviations of vorticity near 500 hPa. Top panel: in operations (from the climatological average of an ensemble of assimilations). Bottom panel: from the ensemble of backgrounds valid for 10 December 2006 at 3 UTC. Unit:* $10^{-5}s^{-1}$.

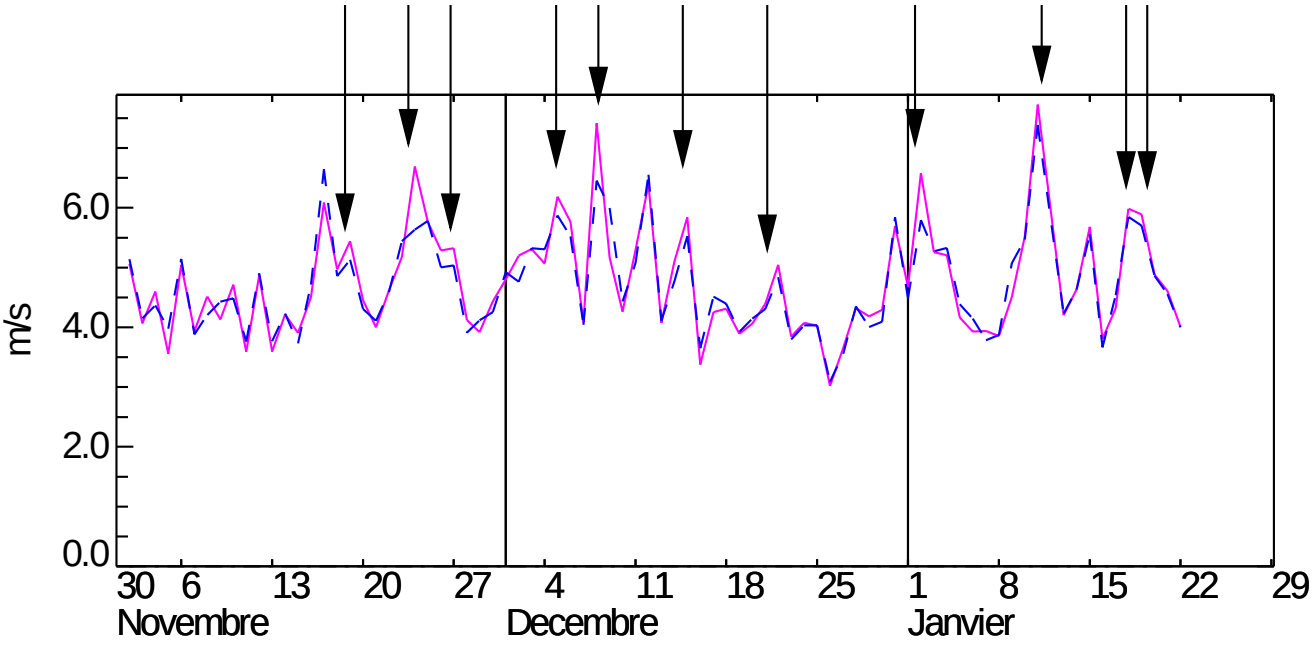


*Figure 8: RMS of 24h forecasts of wind at 500 hPa over Europe, obtained from two different Arpège 4D-Var experiments. Pink full curve: with climatological ensemble sigmab's. Blue dashed curve: with flow-dependent ensemble sigmab's of the day. The vertical black arrows materialize the number of reductions of local RMS peaks.*

The localized nature of these strong modifications implies that it is not expected to obtain a systematic improvement of forecast scores at any place and at any time, but rather a tendency to reduce local errors connected to intense weather systems.

A three-month experiment has thus been carried out, in order to examine the impact of flow-dependent ensemble standard deviations ("of the day"), against the climatological ensemble standard deviations which are currently used in the operational Arpège 4D-Var.

An example of impact is shown in Figure 8 for RMS of 24h forecasts of wind over Europe. While "good" forecasts are not much affected, there is a tendency to reduce the local maxima of RMS. This positive and localized impact in time is consistent with aforementioned expectations from these flow-dependent local modifications of the standard deviations.

A similar tendency has been observed for local areas such as North-America and Australia-New Zealand, while being less visible when scores are averaged over very large domains such as the extratropical Northern Hemisphere. This illustrates that the impact is localized in space (as expected).

These positive local impacts (in space and time) were also found to be larger for wind than for geopotential, in accordance with possible connections to intense weather systems with large wind speeds. This is also consistent with case studies in Kucukkaraca and Fisher (2006) of intense events such as the second French storm.

## 4 Spatial filtering of local correlations

### 4.1 Wavelets as a relevant compromise between two extreme approaches

It may be noticed that there are typically two extreme approaches in correlation modelling.

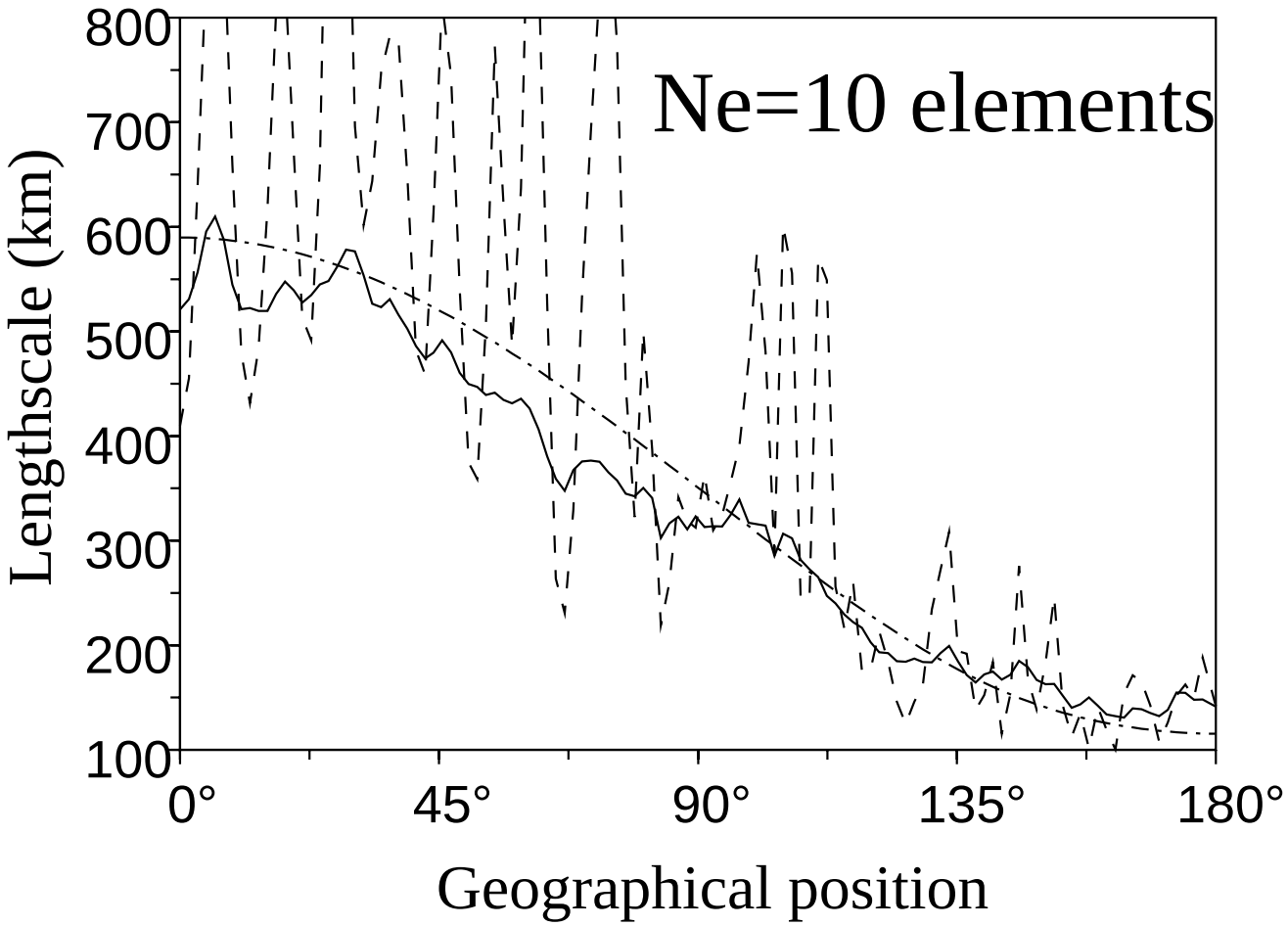


*Figure 9: Geographical variations of the correlation length-scales in a 1D academic case: exact (dash-dotted line), raw 10-member estimate (dashed line), and wavelet 10-member estimate (full line).*

Ensemble Kalman filters are based on local correlation functions, which are calculated independently for each gridpoint. This looks good with respect to the idea to represent a lot of geographical variations, but it also means that a rather large ensemble is needed, in order to have a large statistical sample.

Variational assimilation schemes often use a spectral diagonal approach, which amounts to calculating a global spatial average of the correlation functions. This is rather good with respect to the idea to use a large spatial sample, but it also means homogeneity, and then there are no geographical variations at all.

In this context, an interesting compromise (to combine heterogeneity and an increased sample size) is to use wavelets, in order to calculate a local average of correlations. This potential has been illustrated by Pannekoucke et al (2007), in a simulated 1D academic case, and also in the context of a real ensemble of assimilations.

### 4.2 The spatial structure of sampling noise and its filtering in a simulated framework

Figure 9 corresponds to the 1D academic case. The sinusoide is an example of length-scale map, and the noisy dashed curve is the raw ensemble estimation with 10 members. While the main geographical contrast is captured, there is also a lot of noise, which varies much from one gridpoint to the next one. In particular, the spatial structure of this sampling noise is thus relatively small scale (with higher frequencies than for the signal).

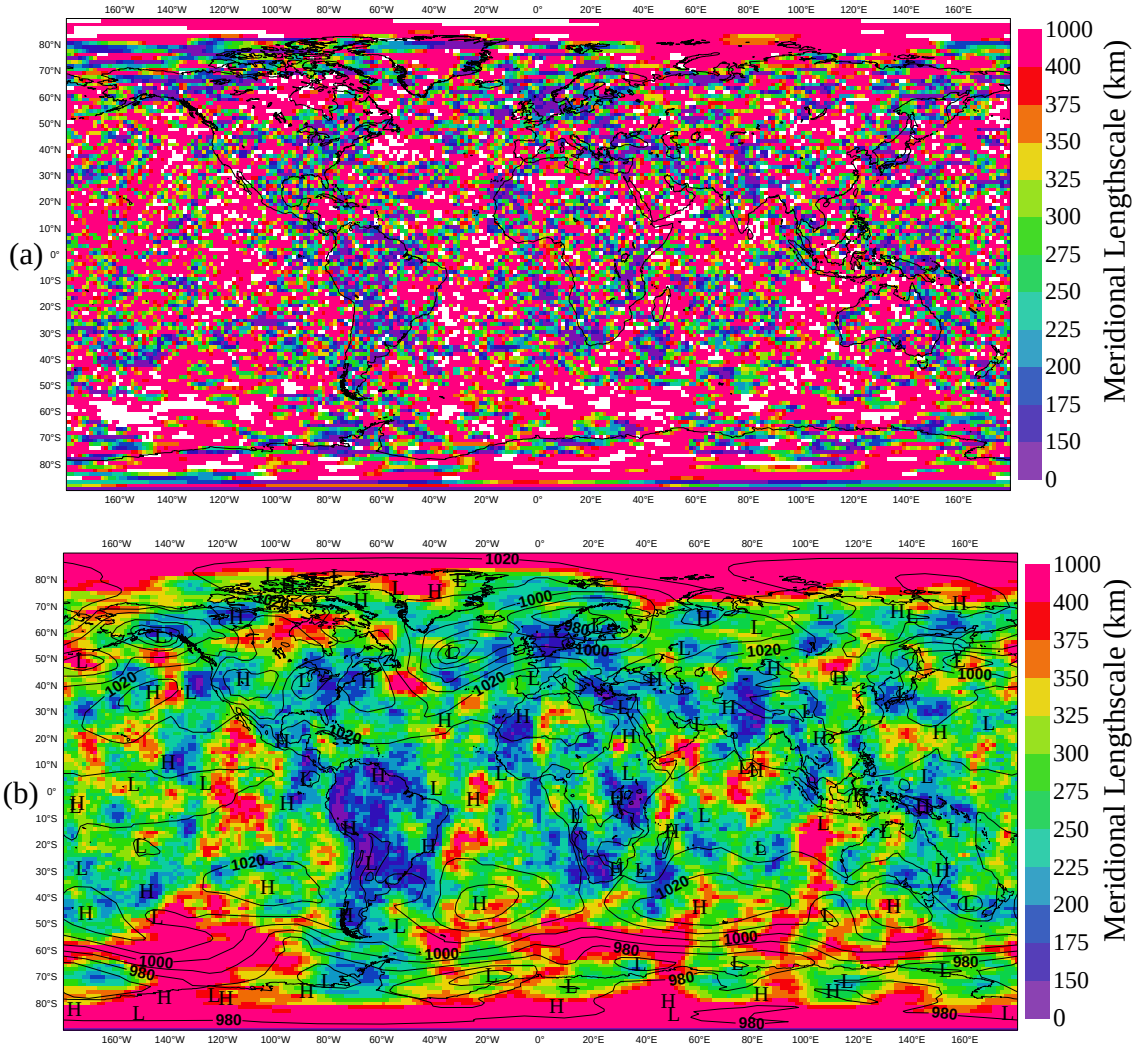


*Figure 10: Meridional length-scales (km) for surface pressure on 10 February 2002 at 12 UTC. Top panel: raw length-scales. Bottom panel: wavelet-implied length-scales, superimposed on the background field of surface pressure.*

The full line is from the wavelet ensemble estimation, still with 10 members. The sampling noise is much smaller, and the main variation is still represented. This illustrates the potential efficiency of the wavelet local averaging.

### 4.3 The spatial structure of sampling noise and its filtering in a real NWP context

This is further illustrated in Figure 10 by a map of the length-scales ”of the day”, from a real 6-member assimilation ensemble. The top panel corresponds to the raw ensemble estimation, which is very noisy, even if a few patterns can be identified.

The bottom panel corresponds to the wavelet ensemble estimation, which is much more structured, for instance with smaller length-scales near the Andes mountains, and small length-scales near the Scandinavian low (and larger length-scales in the Southern hemisphere).

Case studies over several days have been carried out (not shown). They tend to indicate that it is important to consider a real time assimilation ensemble, instead of e.g. a simplified background state dependence, in order

to represent effects of both meteorological processes and data density.

## 5 Conclusions and perspectives: towards optimized flow-dependent covariances

A step-by-step approach has been applied, in order to extract realistic and useful information from an ensemble of variational assimilations. Initially, climatological averages of global covariances and of local standard deviations, from an off-line assimilation ensemble, have been calculated and implemented operationally.

Current work is now devoted to the extraction of flow-dependent information on local standard deviations and correlations, from a real time variational ensemble. Combining such an assimilation ensemble and spatial filtering techniques seems to be a promising way to do this. Standard deviation maps can be easily filtered in spectral space, and a wavelet approach allows the correlation functions to be efficiently filtered.

The spatial filtering is justified by the relatively small scale structure of sampling noise, and it can be optimized objectively with simple statistical techniques. The local spatial averaging allows the sample size to be much increased, because the ensemble size is multiplied by a 2D spatial sample size. Moreover, the spatial filtering is relatively costless. Thus, it may help to reduce the constraint on the required number of ensemble members (to reach a given accuracy).

First impact experiments and comparisons with innovation-based diagnostics are encouraging. A real time ensemble is thus considered to become operational at Météo-France in 2008, to provide flow-dependent background error standard deviations (as a first step). Applications for correlations (using wavelets), assimilation diagnostics and ensemble prediction will be considered too.

## 6 References

Andersson, E. and M. Fisher, 1998: Background errors for observed quantities and their propagation in time. *Proceedings of the ECMWF workshop on Diagnosing Data Assimilation Systems*, 81-89.

Belo Pereira, M. and L. Berre, 2006: The use of an Ensemble approach to study the Background Error Covariances in a Global NWP Model. *Mon.Wea.Rev.*, **134**, 2466-2489.

Berre, L., S.E., Ştefănescu, and M. Belo Pereira, 2005: The representation of the analysis effect in three error simulation techniques. *Tellus*, **58A**, 196-209.

Bishop, C.H., B. J. Etherton and S. J. Majumdar, 2001: Adaptive Sampling with the Ensemble Transform Kalman Filter. Part I: Theoretical Aspects. *Mon. Wea. Rev.*, **129**, 420-436.

Buehner, M., 2005: Ensemble-derived stationary and flow-dependent background-error covariances: Evaluation in a quasi-operational NWP setting. *Q. J. Roy. Meteor. Soc.*, **131**, 1013 - 1043.

Courtier, P. and J.F. Geleyn, 1988: A global numerical weather prediction model with variable resolution: Application to the shallow-water equations. *Quart. J. Roy. Meteor. Soc.*, **114**, 1321-1346.

Courtier, P., Andersson, E., Heckley, W., Pailleux, J., Vasiljevic, D., Hamrud, M., Hollingsworth, A., Rabier, F. and Fisher, M., 1998: The ECMWF implementation of three dimensional variational assimilation (3D-Var). Part I: Formulation. *Quart. J. Roy. Meteorol. Soc.*, **124**, 1783-1808.

Daley, R., 1992 : Estimating model-error covariances for application to atmospheric data assimilation. *Mon. Wea. Rev.*, **120**, 1735-1746.

Desroziers, G., L. Berre, B. Chapnik, and P. Poli, 2005: Diagnosis of observation, background and analysis error statistics in observation space. *Quart. J. Roy. Meteorol. Soc.*, **131**, 3385-3397.

Desroziers, G., L. Berre, O. Pannekoucke, S.E. Ştefănescu, P. Brousseau, L. Auger and B. Chapnik, 2007: Flow-dependent error covariances from variational assimilation ensembles on global and regional domains. Proceedings of the SRNWP workshop on high resolution data assimilation. To appear in a Hirlam technical report.

Fisher, M. and P. Courtier, 1995: Estimating the covariance matrices of analysis and forecast error in variational data assimilation. *ECMWF technical memorandum* **220**, 28 pages.

Fisher, M., 2003: Background error covariance modelling. *Proceedings of the ECMWF Seminar on Recent developments in data assimilation for atmosphere and ocean, 8-12 September 2003*, 45-63.

Houtekamer, P.L., Lefaivre, L., Derome, J., Ritchie, H. and Mitchell, H.L., 1996: A System Simulation Approach to Ensemble Prediction. *Mon. Wea. Rev.*, **124**, 1225-1242.

Kucukkaraca, E. and M. Fisher, 2006: Use of analysis ensembles in estimating flow-dependent background error variances. ECMWF Technical Memorandum, **492**. European Centre for Medium-range Weather Forecasts (ECMWF), Reading, UK.

Lorenc, A.C., 2003: The potential of the ensemble Kalman filter for NWP - a comparison with 4D-Var. *Quart. J. Roy. Meteor. Soc.*, **129**, 3183 - 3203.

Monin, A.S., and Yaglom, A.M., 1971: Statistical fluid mechanics: mechanics of turbulence. Vol. 1. The MIT Press. Cambridge (USA).

Pannekoucke, O., L. Berre and G. Desroziers, 2007: Filtering properties of wavelets for the local background error correlations. *Q. J. Roy. Meteor. Soc.*, **133**, 363 - 379.

Parrish, D.F. and J.C. Derber, 1992: The National Meteorological Center's spectral statistical interpolation analysis system. *Mon. Wea. Rev.*, **120**, 1747-1763.

Rabier, F., Mc Nally, A., Andersson, E., Courtier, P., Undén, P., Eyre, J., Hollingsworth, A., Bouttier, F., 1998: The ECMWF implementation of three dimensional variational assimilation (3D-Var). Part II: Structure functions. *Quart. J. Roy. Meteor. Soc.*, **124**, 1809-1829.